AMERICAN SOCIETY FOR MICROBIOLOGY | Journal of Virology

Glutathione Depletion Is Linked with Th2 Polarization in Mice with a Retrovirus-Induced Immunodeficiency Syndrome, Murine AIDS: Role of Proglutathione Molecules as Immunotherapeutics

Serena Brundu,[a] Linda Palma,[a] Giusi Giada Picceri,[a] Daniela Ligi,[a] Chiara Orlandi,[a] Luca Galluzzi,[a] Laura Chiarantini,[a] Anna Casabianca,[a] Giuditta Fiorella Schiavano,[a] Martina Santi,[a] Ferdinando Mannello,[a] Kathy Green,[b] Michaël Smietana,[c] Mauro Magnani,[a] Alessandra Fraternale[a]

Department of Biomolecular Sciences, University of Urbino Carlo Bo, Urbino, PU, Italy[a]; Department of Microbiology and Immunology, Geisel School of Medicine at Dartmouth, Lebanon, New Hampshire, USA[b]; Institut des Biomolécules Max Mousseron, UMR 5247, CNRS, Université de Montpellier, Montpellier, France[c]

ABSTRACT

Injection of the LP-BM5 murine leukemia virus into mice causes murine AIDS, a disease characterized by many dysfunctions of immunocompetent cells. To establish whether the disease is characterized by glutathione imbalance, reduced glutathione (GSH) and cysteine were quantified in different organs. A marked redox imbalance, consisting of GSH and/or cysteine depletion, was found in the lymphoid organs, such as the spleen and lymph nodes. Moreover, a significant decrease in cysteine and GSH levels in the pancreas and brain, respectively, was measured at 5 weeks postinfection. The Th2 immune response was predominant at all times investigated, as revealed by the expression of Th1/Th2 cytokines. Furthermore, investigation of the activation status of peritoneal macrophages showed that the expression of genetic markers of alternative activation, namely, Fizz1, Ym1, and Arginase1, was induced. Conversely, expression of inducible nitric oxide synthase, a marker of classical activation of macrophages, was detected only when Th1 cytokines were expressed at high levels. *In vitro* studies revealed that during the very early phases of infection, GSH depletion and the downregulation of interleukin-12 (IL-12) p40 mRNA were correlated with the dose of LP-BM5 used to infect the macrophages. Treatment of LP-BM5-infected mice with *N*-(*N*-acetyl-L-cysteinyl)-*S*-acetylcysteamine (I-152), an *N*-acetyl-cysteine supplier, restored GSH/cysteine levels in the organs, reduced the expression of alternatively activated macrophage markers, and increased the level of gamma interferon production, while it decreased the levels of Th2 cytokines, such as IL-4 and IL-5. Our findings thus establish a link between GSH deficiency and Th1/Th2 disequilibrium in LP-BM5 infection and indicate that I-152 can be used to restore the GSH level and a balanced Th1/Th2 response in infected mice.

IMPORTANCE

The first report of an association between Th2 polarization and alteration of the redox state in LP-BM5 infection is presented. Moreover, it provides evidence that LP-BM5 infection causes a decrease in the thiol content of peritoneal macrophages, which can influence IL-12 production. The restoration of GSH levels by GSH-replenishing molecules can represent a new therapeutic avenue to fight this retroviral infection, as it reestablishes the Th1/Th2 balance. Immunotherapy based on the use of pro-GSH molecules would permit LP-BM5 infection and probably all those viral infections characterized by GSH deficiency and a Th1/Th2 imbalance to be more effectively combated.

Infection with the LP-BM5 murine leukemia virus causes a profound and broad immunodeficiency in susceptible mouse strains, such as C57BL/6 (B6) mice. This disease is known as murine AIDS (MAIDS) and is characterized by early polyclonal T- and B-cell activation, splenomegaly, lymphadenopathy, hypergammaglobulinemia, decreased T- and B-cell responses, increased susceptibility to opportunistic pathogens, and the development of terminal B-cell lymphomas and neurological dysfunctions (1–4). MAIDS is characterized by physiological abnormalities which are similar to those observed in the early stages of human AIDS. Hence, this model may be used to provide insights into the immunosuppressive changes characterizing human retrovirus infections, which in turn could lead to new antiretroviral drugs and new pharmacological approaches (5–10).

LP-BM5-infected mice develop functional and phenotypic changes in leukocyte populations, leading to a profound immunodeficiency and a shift in cytokine profiles from a Th1 to a Th2 phenotype (11–15). T-cell differentiation from naive Th0 cells into Th1 or Th2 cells depends on the cytokine milieu induced during the innate activation of macrophages (16); for example, interleukin-12 (IL-12) and tumor necrosis factor alpha (TNF-α) activate Th1 T cells, whereas the IL-10 cytokine favors Th2 T-cell development (17). The glutathione-redox balance in antigen-presenting cells (APC) has a critical role in the development of innate immune responses. Low levels of reduced glutathione (GSH) decrease the level of secretion of IL-12 and lead to the polarization

Received 4 April 2016 **Accepted** 19 May 2016

Accepted manuscript posted online 25 May 2016

Citation Brundu S, Palma L, Picceri GG, Ligi D, Orlandi C, Galluzzi L, Chiarantini L, Casabianca A, Schiavano GF, Santi M, Mannello F, Green K, Smietana M, Magnani M, Fraternale A. 2016. Glutathione depletion is linked with Th2 polarization in mice with a retrovirus-induced immunodeficiency syndrome, murine AIDS: role of proglutathione molecules as immunotherapeutics. J Virol 90:7118–7130. doi:10.1128/JVI.00603-16.

Editor: S. R. Ross, University of Illinois at Chicago College of Medicine

Address correspondence to Alessandra Fraternale, alessandra.fraternale@uniurb.it.

from the Th1 cytokine profile toward Th2 response patterns; on the contrary, high levels of GSH favor a Th1 response (17, 18). Th1 cells, which produce gamma interferon (IFN-γ) and IL-2, evoke cell-mediated immunity. Th2 cells, which produce IL-4, IL-5, IL-6, IL-9, IL-10, and IL-13, evoke strong antibody responses (including those of the IgE class) (19).

The Th1 immune response is known to be suppressed during infections by different pathogens, such as HIV, *Leishmania*, and *Mycobacterium tuberculosis* (20–22). Interestingly, studies also show that patients with AIDS or tuberculosis have an altered glutathione balance (23–25), and HIV-associated disturbances in GSH have been associated with impaired survival (26). The shift toward a Th2-dominant state and the deficiency in the induction of specific Th1 cells observed during infections may compromise the ability of the host to protect against intracellular pathogens. Undoubtedly, several factors are involved in the functional alterations associated with cell-mediated immunity; however, GSH depletion appears to be an important feature which can contribute to the imbalance in the Th1/Th2 response (20–26).

In the present study, to evaluate whether GSH depletion could be involved in the progression of MAIDS, GSH and cysteine contents were studied in spleen and lymph nodes, where $CD4^+$ T cells are central to the induction and progression of both B- and T-cell abnormalities in MAIDS (27). Moreover, it has been reported that LP-BM5 infection is accompanied by a pancreatitis-like injury (28) and by central nervous system (CNS) damage (29–31). Hence, to investigate whether the thiol content could play a role in the alterations of these organs, GSH and cysteine levels were also measured in the pancreas and brain.

The Th1/Th2 cytokine profile was also investigated when thiol measurements were made. Moreover, it is known that the cytokine environment influences the development of macrophages into different subsets (32). Classically activated macrophages (CAMϕ), induced by IFN-γ and lipopolysaccharide (LPS), are important players in the elimination of various pathogens. Th2 immune response mediators, i.e., IL-4 and IL-13, antagonize CAMϕ and induce the development of alternatively activated macrophages (AAMϕ) (32).

AAMϕ are associated with Fizz1, Ym1, and Arginase1 (Arg1) expression, suggesting that these genes can constitute useful markers for the identification of AAMϕ. Indeed, they have been found to be abundantly expressed in peritoneal macrophages after infection with Th2-inducing pathogens (33–35). Therefore, we focused on the identification of genes that are differentially expressed in AAMϕ to correlate the recruitment of AAMϕ with a polarized Th2 immune response in this model. At all the time points investigated, a redox imbalance consisting of GSH and/or cysteine depletion was found in several organs. Moreover, a prevalent Th2 immune response associated with an alternative pathway of macrophage activation was found to characterize LP-BM5 infection. The treatment of LP-BM5-infected mice with *N*-(*N*-acetyl-L-cysteinyl)-*S*-acetylcysteamine (I-152), a prodrug of *N*-acetyl-cysteine (NAC) and beta-mercaptoethylamine (cysteamine), which was already successfully used both as an antiviral and as an immunomodulator (36–39), could restore the intraorgan GSH content and a balanced Th1/Th2 response. These data show that, similarly to what happens in other viral infections (20, 26, 40–44), a Th1/Th2 imbalance can be mediated by GSH-dependent mechanisms in MAIDS as well. Consequently, the restoration of intracellular GSH levels can represent the basis for a new therapeutic intervention for this pathology and for all those characterized by GSH deficiency and downregulation of the Th1 immune response.

MATERIALS AND METHODS

Ethics statement. In the first series of experiments, the mice were housed and treated in compliance with the recommendations in the *Guide for the Care and Use of Laboratory Animals* (45) and those of the Health Ministry of Italy, Law 116, 1992. Experiments were done with the approval of the Committee on the Ethics of Animal Experiments of the University of Urbino Carlo Bo.

In the second series of experiments, the mice were housed and treated in compliance with the recommendations in the *Guide for the Care and Use of Laboratory Animals* (45) and those of the Health Ministry of Italy, Law 26/2014, and the experiments were done upon authorization number 279/2015-PR by the Health Ministry of Italy.

Mice. Four-week-old female C57BL/6 (B6) mice were purchased from Charles River Laboratories Italy and housed in the animal facility of the Department of Biomolecular Sciences (University of Urbino), which is approved by the Health Ministry of Italy.

LP-BM5 virus inoculation. The LP-BM5 viral mixture was prepared by coculturing G6 cells with uninfected SC-1 cells as previously described (4). C57BL/6 mice were infected by two successive intraperitoneal (i.p.) injections at 24-h intervals of 100 μl of the LP-MB5 murine leukemia virus stock, in which each injection contained 0.25 units of reverse transcriptase (RT). At 2, 5, and 9 weeks after virus inoculation, 5 uninfected mice and 5 LP-BM5-infected mice were sacrificed. In a second experiment, the uninfected and infected mouse groups described above were replicated and two infected groups receiving either I-152 or placebo were added.

Treatment of LP-BM5-infected mice with I-152. Mice were infected as described above. At 1 h after each virus inoculation, 15 mice received i.p. injections of I-152 (30 μmol/mouse in 200 μl of 0.9% NaCl) or placebo (200 μl 0.9% NaCl). Treatments were repeated three times a week for a total of 9 weeks. I-152 was synthesized as previously described (36).

Quantification of thiol species in mouse organs and peritoneal macrophages. The thiol content in the spleen, lymph nodes, pancreas, and brain of uninfected or infected mice was determined at 2, 5, and 9 weeks after virus inoculation by a high-performance liquid chromatography (HPLC) method which has recently been validated according to U.S. and European standards (46). Briefly, a portion of each organ (10 to 20 mg) was immersed in 500 μl of precipitating solution (100 ml containing 1.67 g of glacial *meta*-phosphoric acid, 0.2 g of disodium EDTA, 30 g of NaCl), and then it was homogenized and sonicated. The sample was kept in ice for 10 min and then centrifuged at 12,000 × *g* for 10 min at 4°C. Fifteen microliters of 0.3 M Na_2HPO_4 was added to 60 μl of the acid extract, and immediately after that, 45 μl 5,5′-dithio-bis-(2-nitrobenzoic acid) (DTNB) was added. DTNB solution was prepared by dissolving 20 mg of DTNB in 100 ml of sodium citrate solution (1%, wt/vol). The mixture was stirred for 1 min, left at room temperature for another 5 min, and, finally, used for quantification of cysteine and GSH by HPLC. A Teknokroma Tracer Excel 120 octadecyl-silica A (ODS-A) column (particle size, 5 μm; 15 cm by 0.46 cm) protected by a guard column was used in these studies. The mobile phase consisted of 10 mM KH_2PO_4 solution, pH 6.0 (buffer A), and buffer A containing 60% (vol/vol) acetonitrile (buffer B). The elution conditions were as follows: 10 min of 100% buffer A, followed by an increase to 100% buffer B over 15 min; this condition was maintained for 5 min. The gradient was returned to 100% buffer A over 3 min. The flow rate was 1 ml/min, the injection volume was 50 μl, and detection was at 330 nm.

Determination of the amount of thiol in peritoneal macrophages was performed as previously described (47). The removed macrophages were immediately lysed with 100 μl of lysis buffer (0.1% Triton X-100, 0.1 M Na_2HPO_4, 5 mM EDTA, pH 7.5). Thereafter, 15 μl of 0.1 N HCl and 140 μl of precipitating solution were added. After centrifugation, the super-

natants were collected, 25% (vol/vol) 0.3 M Na_2HPO_4 was added, and immediately after that 10% (vol/vol) DTNB was added. Then the samples were submitted to the same procedure described above and analyzed by HPLC as described above for the organ tissue samples.

Quantification of GSSG in organs. The spleen, lymph nodes, pancreas, and brain of uninfected or infected mice were evaluated for the oxidized form of glutathione (GSSG) at 2, 5, and 9 weeks after virus inoculation.

A portion of organ tissue (20 to 40 mg) was put into an Eppendorf tube containing 500 μl of 20% *meta*-phosphoric acid. The sample was homogenized and then sonicated as described above for the quantification of thiol species in the organs. After centrifugation, the acid extracts were neutralized through 1 M Tris-HCl and used for measurement of the amount of GSSG, which was performed spectrophotometrically as previously described (48).

Cytokine assay. The production of Th1 cytokines (IL-2, IL-12, IFN-γ) and Th2 cytokines (IL-5, IL-4, IL-10) from splenocytes obtained from uninfected or infected mice was determined. Briefly, spleen lymphocytes were seeded in duplicate at a density of 5×10^5 per well in 96-well tissue culture plates in 200 μl of RPMI 1640 complete medium (10% heat-inactivated fetal bovine serum, 100 U/ml penicillin, 100 μg/ml streptomycin). They were incubated for 72 h at 37°C in a 5% CO_2 atmosphere. The supernatants were collected and stored at −80°C until analysis. The cytokines were determined by a multiplex biometric enzyme-linked immunosorbent assay (ELISA)-based immunoassay containing fluorescently dyed magnetic beads covalently conjugated with a monoclonal antibody specific for the target protein according to the manufacturer's instructions (Bio-Plex; Bio-Rad Laboratories, Inc., Hercules, CA, USA). Soluble molecules were measured using a commercially available kit (a Pro mouse cytokine Th1/Th2 8-plex panel including IL-2, IL-4, IL-5, IL-10, IL-12 p70, granulocyte-macrophage colony-stimulating factor [GM-CSF], IFN-γ, and TNF-α).

Each experiment was performed at least in duplicate according to the manufacturer's instructions. The levels of all cytokines were determined using a Bio-Plex 200 array reader, which is based on Luminex X-Map technology (Bio-Rad Laboratories, Hercules, CA, USA) and which detects and quantifies multiple targets in a 96-well plate with a low volume (50 μl) of a single fluid sample. The interleukin concentrations (expressed as picograms per milliliter) were calculated by use of a standard curve and software provided by the manufacturer (Bio-Plex manager software, v.6.1).

Spleen expression profile. The expression of 11 cytokines in spleens from uninfected and infected mice was assessed at 2, 5, and 9 weeks after virus inoculation using a custom RT^2 profiler PCR array (SABiosciences). The genes in the PCR array, including two housekeeping genes and three internal controls, are listed in Table 1.

Total RNA was extracted from 8 to 10 mg of spleen tissue preserved in RNAlater solution (Qiagen) using an RNeasy minikit (Qiagen). The RNA was quantified using a spectrophotometer (catalog number UV-2401PC; Shimadzu). The cDNA was synthesized from 0.8 μg of total RNA using an RT^2 first-strand cDNA synthesis kit (Qiagen) according to the manufacturer's instructions. Real-time PCRs (total volume, 20 μl) were carried out in a custom RT^2 Profiler PCR array (100-well disk format) with RT^2 SYBR green ROX FAST master mix (Qiagen) using a Rotor-Gene 6000 real-time PCR machine (Corbett Life Science). The PCR protocol consisted of 1 cycle of 10 min at 95°C, followed by 40 cycles of denaturation at 95°C for 15 s and annealing and extension at 60°C for 1 min. The cDNA from uninfected mice was used as a calibrator. Data analysis was based on the $\Delta\Delta C_T$ threshold cycle (C_T) method: the raw data were normalized using reference housekeeping genes, and the analysis was performed using web-based RT^2 Profiler PCR array data analysis software (SABiosciences).

Determination of IgE in mouse plasma. At 2, 5, and 9 weeks after virus inoculation, plasma IgE levels were determined by ELISA using a kit from Bethyl Laboratories, Inc. (Montgomery, TX), according to the manufacturer's instructions. A standard curve for IgE was obtained using the recombinant standard protein provided by the manufacturer.

TABLE 1 PCR array format[a] and genes for which samples were tested

Position	Gene symbol	Gene description	Gene RefSeq accession no.
1	IFNG	Gamma interferon	NM_008337
2	Il10	Interleukin-10	NM_010548
3	Il2	Interleukin-2	NM_008366
4	Il27	Interleukin-27	NM_145636
5	Il4	Interleukin-4	NM_021283
6	Il5	Interleukin-5	NM_010558
7	Irf1	Interferon regulatory factor 1	NM_008390
8	Nfkb1	Nuclear factor of kappa light polypeptide gene enhancer in B cells 1, p105	NM_008689
9	Stat1	Signal transducer and activator of transcription 1	NM_009283
10	Tnf	Tumor necrosis factor	NM_013693
11	Il12b	Interleukin-12b	NM_008352
12	B2M	Beta-2-microglobulin	NM_009735
13	Gapdh	Glyceraldehyde-3-phosphate dehydrogenase	NM_008084
14	MGDC	Mouse genomic DNA contamination control	
15	RTC	Reverse transcription control	
16	PPC	Positive PCR control	

[a] The PCR array format consisted of 16 genes and 6 samples per disk.

Murine peritoneal macrophage isolation. Peritoneal exudate cells of B6 mice were obtained by peritoneal lavage as previously described (47). Macrophages were incubated for 24 h in 35-mm-diameter dishes with RPMI 1640 medium (Sigma) supplemented with 10% heat-inactivated fetal bovine serum (EuroClone), 2 mM L-glutamine, 100 U/ml penicillin, and 100 μg/ml streptomycin (Sigma) and then processed differently according to the determinations that were to be made.

Peritoneal macrophage expression profile. To study the macrophage expression of Fizz1 (NM_020509), Ym1 (NM_009892), Arg1 (NM_007482), and inducible nitric oxide synthase (iNOS) (NM_010927) in uninfected and infected mice, peritoneal macrophages, isolated and cultured as described above, were lysed in phenol-chloroform-isoamyl alcohol (25:24:1) and collected in microcentrifuge tubes. Total RNA from peritoneal macrophages was extracted as described by Sambrook et al. (49) and subsequently processed for contaminant DNA removal with a DNase-free kit (Thermo Fisher Scientific, Waltham, MA, USA). The RNA concentration was evaluated with a NanoDrop ND-1000 spectrophotometer (NanoDrop Technologies, Wilmington, DE, USA), and 0.5 μg of the total RNA was utilized for cDNA synthesis in a 10-μl reaction mix using a PrimeScript RT master mix (TaKaRa). Real-time PCR analysis was performed in a 7500 real-time PCR system (Applied Biosystems) with the software package SDS (v.1.4.0). The PCR mixtures were assembled in a 25-μl volume using 2× master mix from a Hot-Rescue real-time PCR kit-SYBR green (SG) (Diatheva, Fano, Italy) and 360 nM each primer. Primer oligonucleotides were purchased from Sigma-Aldrich (St. Louis, MO, USA). Primer sequences were as follows: for actin, forward primer 5′-TCC ACC CGC GAG CAC A-3′ and reverse primer 5′-ACA TGC CGG AGC CGT TGT-3′; for Arg1, forward primer 5′-TCA ACA CTC CCC TGA CAA C-3′ and reverse primer 5′-CAG ATA TGC AGG GAG TCA CC-3′; for Fizz1, forward primer 5′-TTG CCA ATC CAG CTA ACT AT-3′ and reverse primer 5′-CAG TGG TCC AGT CAA CGA-3′; for iNOS, forward primer 5′CCC TTC CGA AGT TTC TGG CAG C3′ and reverse primer 5′CCC TTC CGA AGT TTC TGG CAG C3′; and for Ym1, forward primer 5′-ACA GGT CTG GCA ATT CTT CT-3′ and reverse primer 5′-AAA GGC ATA GAT CAG GTG AGT A-3′. For each sample, three replicates corresponding to 10 ng of total RNA were run. Thermal cycling was per-

formed as follows: 10 min at 95°C; 45 cycles of denaturation at 95°C for 15 s, annealing at either 61°C (Actin, Ym1, Arg1) or 55°C (Fizz1, iNOS) for 15 s, and extension at 72°C for 35 s. At the end of the PCR cycles, a melting curve was generated to verify the specificity of the PCR products. The relative amounts of mRNAs for selected target genes were calculated according to the $2^{-\Delta\Delta CT}$ comparative method using the gene for β-actin (GenBank accession number NM_007393) as a reference; infected mice were considered calibrators (50).

***In vitro* infection of murine peritoneal macrophages with LP-BM5.** Murine peritoneal macrophages, isolated and cultured as described above, were infected with LP-BM5 retroviral complex containing either 0.5 or 1.0 unit of RT. After virus removal, the cells were washed twice, and at 3 and 6 days postinfection, the DNA content of the etiologic agent in the LP-BM5 mixture, that is, replication-defective virus (BM5d) (51), IL-12 p40 mRNA expression, and thiol species were quantified.

Quantification of IL-12 p40 mRNA in peritoneal macrophages infected with LP-BM5. The IL-12 p40 mRNA in murine peritoneal macrophages infected *in vitro* was quantified as previously described (47). Briefly, total RNA was isolated from about 2.5×10^5 macrophages using an RNeasy minikit (Qiagen), and 0.8 μg was used for cDNA synthesis (RT^2 first-strand cDNA synthesis kit; Qiagen) according to the manufacturer's instructions. Real-time PCRs (total volume, 50 μl) were performed with the master mix from the Hot-Rescue real-time PCR kit-SG (Diatheva, Fano, Italy), a 7500 real-time PCR instrument (Applied Biosystems), and the Sequence detection system software package (v.1.4.0). mRNA levels were normalized to 100 ng of total RNA.

Quantification of BM5d DNA in peritoneal macrophages infected with LP-BM5 and in organs of LP-BM5-infected mice. BM5d DNA was quantified in peritoneal macrophages infected *in vitro* with LP-BM5 and in the spleen, lymph nodes, pancreas, and brain of LP-BM5-infected mice.

At 3 and 6 days after LP-BM5 infection, cellular DNA was isolated from about 2.5×10^5 macrophages using a QIAamp DNA minikit (Qiagen) according to the manufacturer's instructions.

Total cellular DNA was isolated from frozen tissue (10 to 20 mg) and purified by the lysis-phenol method (51). The DNA concentration was evaluated with a NanoDrop ND-1000 spectrophotometer (NanoDrop Technologies, Wilmington, DE, USA), and the ratios of that absorbance at 260 nm/280 nm and absorbance at 260 nm/230 nm were used to control the quality; all samples had ratios of about 1.8 and 2.0, respectively, and were accepted as pure DNA. BM5d DNA quantification was performed by SYBR green I real-time PCR, as previously described (51). The reactions were carried out on an Applied Biosystems 7500 real-time PCR system with a final volume of 50 μl, using 2× master mix from the Hot-Rescue real-time PCR kit-SG (Diatheva, Fano, Italy) and 50 to 100 ng of DNA. The copy number of BM5d DNA was calculated by interpolation from the experimentally determined standard curve and was normalized to 100 ng of DNA.

Statistical analysis. Statistical analysis was performed using the Mann-Whitney test for all the parameters, with the exception of determinations in murine macrophages infected *in vitro* with LP-BM5, for which statistical analysis was performed by the Student *t* test. A *P* value of less than 0.05 was considered significant.

RESULTS

GSH and cysteine levels in organs of LP-BM5-infected mice. To assess whether LP-BM5 infection caused GSH depletion, GSH and cysteine levels in the lymphoid organs (spleen and lymph nodes), known to be the sites where viral loads are higher (51), were determined. In mice with MAIDS, pancreatic lesions of the exocrine system with a predominance of infiltrating Th2 cells have been described (28); moreover, CNS damage and cognitive deficits develop concurrently with the immunodeficiency (29–31). Hence, the thiol content in the pancreas and brain was also analyzed. A decrease in the content of thiol species was observed in all organs (Fig. 1), in particular, in spleen and lymph nodes, as expected, given the higher viral load found in these organs (data not shown). Specifically, we observed that in infected mice, (i) the GSH content in the spleen was significantly depleted at 5 and 9 weeks postinfection and the amount of cysteine was significantly lower at all time points studied; (ii) the GSH content in the lymph node showed a significant decrease at 5 and 9 weeks postinfection, while noteworthy differences in cysteine levels were not recorded; (iii) the levels of GSH in the pancreas were unchanged, while the cysteine content was significantly decreased at 5 weeks postinfection; and (iv) the content of GSH in the brain showed a significant decrease at 5 weeks postinfection, and the cysteine content was always unchanged.

The GSSG content was evaluated in all organs, but significant differences were not found when these values were compared with those in the organs of uninfected mice (data not shown).

Expression of Th1 and Th2 cytokines in LP-BM5-infected mice. The expression of Th2 (IL-5, IL-4, IL-10) and Th1 (IL-2, IL-12, IFN-γ) cytokines as well as of TNF-α and GM-CSF was investigated at 2, 5, and 9 weeks after virus inoculation. To this end, both spleen mRNA and proteins secreted in the supernatants of unstimulated spleen cells obtained from uninfected mice or infected mice were analyzed (Fig. 2).

Quantitative analysis revealed that all cytokines were detectable in all mice, including uninfected ones. Regarding the comparison of uninfected and infected mice, at 2 weeks postinfection (Fig. 2A, white bars), cytokine analysis showed that the concentrations of all the cytokines involved in the Th1/Th2 response were statistically significantly increased in infected mice compared to those in uninfected animals. Specifically, IL-5 levels showed a 100-fold increase; IL-4 and IL-2 levels were about 10-fold higher; and IL-10, IL-12, and IFN-γ levels were almost 2-fold higher.

At 5 weeks postinfection (Fig. 2A, black bars), the levels of IL-5, IL-4, and IL-2 released into the culture medium from spleen cells of infected mice were about 40-, 15-, and 8-fold higher, respectively, than those measured for uninfected mice. On the other hand, the levels of IL-10, IL-12, and IFN-γ were not statistically significantly different from those found in uninfected mice.

At both 2 and 5 weeks, the concentrations of TNF-α and GM-CSF measured in infected mice were not significantly different from those measured in uninfected animals.

Real-time PCR analysis of cDNA from the spleens of uninfected and infected mice confirmed this trend of cytokine production, although to a lesser extent. It is noteworthy that the levels of IL-5 transcripts measured in the infected animals were significantly higher than those measured in the uninfected animals at all the times studied (Fig. 2B).

The results obtained at 9 weeks postinfection were comparable to those obtained at 5 weeks postinfection (data not shown).

IgE levels in LP-BM5-infected mice. Quantification of IgE in plasma showed that IgE levels increased significantly in infected mice compared to those in uninfected animals at both 2 and 5 weeks postinfection (Fig. 3). At 9 weeks postinfection, differences between the two groups were not found (data not shown).

Expression of genetic markers of macrophage activation in LP-BM5-infected mice. It has been reported that Th2-polarizing cytokines also prompt macrophages to have an alternative activation profile. In particular, AAMϕ express a peculiar set of genes in mice, including Arg1, Fizz1, and Ym1 (33–35). Therefore, expression of the mRNA of these polarization markers by peritoneal

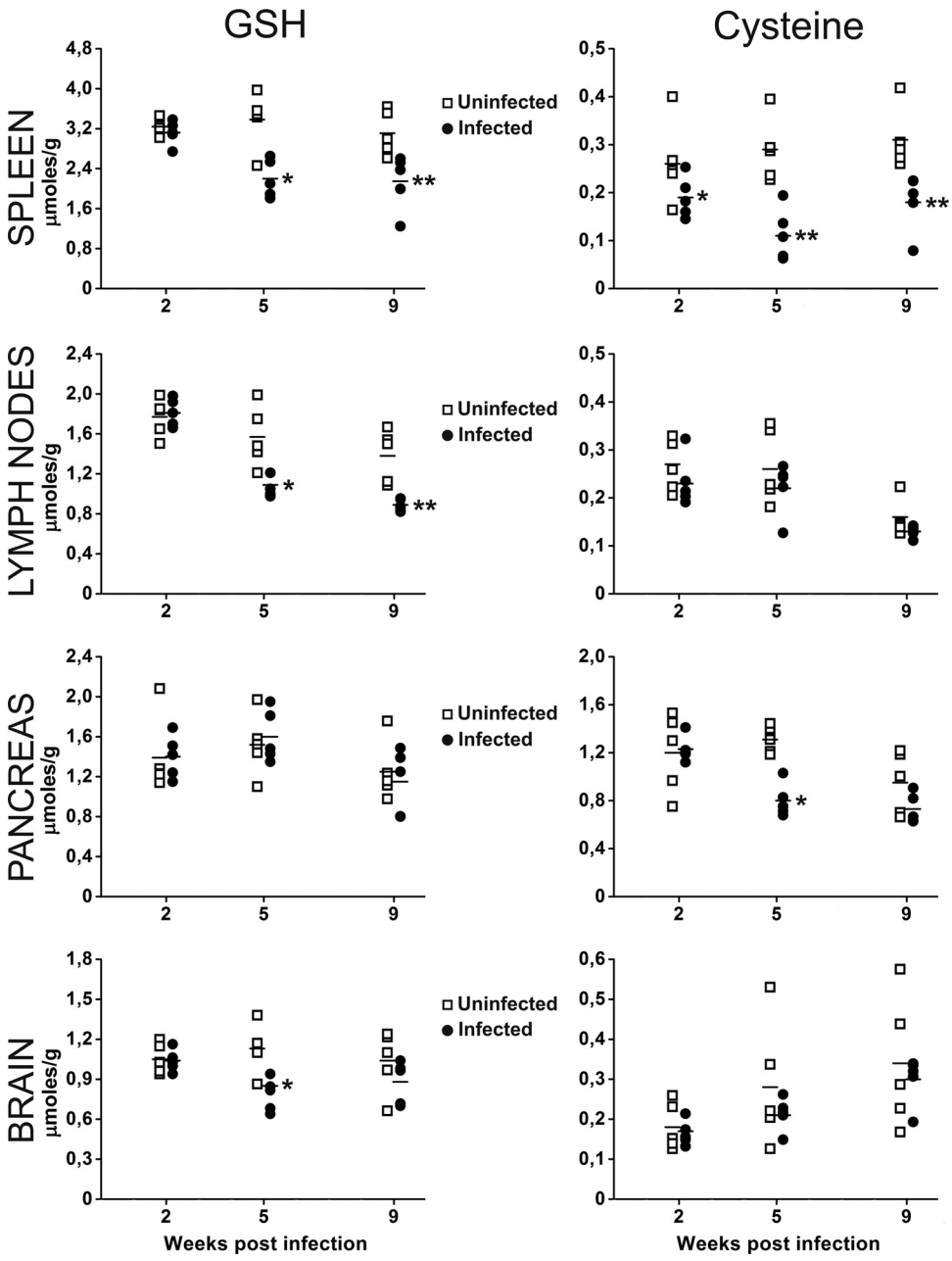

FIG 1 Decreased GSH and cysteine levels in the organs of LP-BM5-infected mice. GSH (left) and cysteine (right) levels were quantified in the spleen, lymph nodes, pancreas, and brain of uninfected or infected mice at 2, 5, and 9 weeks after virus inoculation. Mouse infection and the methods used for determination of GSH and cysteine levels are described in Materials and Methods. *, $P < 0.05$ versus uninfected mice at the same time point; **, $P < 0.01$ versus uninfected mice at the same time point.

macrophages from uninfected and infected mice was compared (Fig. 4). Indeed, Ym1, which was expressed at very low levels in the controls, underwent a robust induction at all the time points tested. Arg1 was also significantly upregulated at 2 and 9 weeks postinfection, although to a lesser extent than Ym1. On the other hand, Fizz1 showed the same expression levels in both control and infected mice. Nonetheless, the alternative polarization profile of macrophages from infected mice was highlighted by the down-modulation of iNOS expression. Indeed, at 2 weeks postinfection, we observed iNOS expression in 3 out of 5 mice, while it remained undetectable at subsequent postinfection time points and in most uninfected controls at all the time points.

Thiol content and expression of IL-12 p40 mRNA in murine peritoneal macrophages infected with LP-BM5. The relationship between the intracellular thiol content, IL-12 p40 mRNA expression, and virus load during the early phases of infection was investigated. To this aim, murine peritoneal macrophages were infected *in vitro* with 0.5 and 1 RT unit of LP-BM5, and GSH and cysteine contents as well as the level of IL-12 p40 mRNA expression were determined at 3 and 6 days postinfection. The results

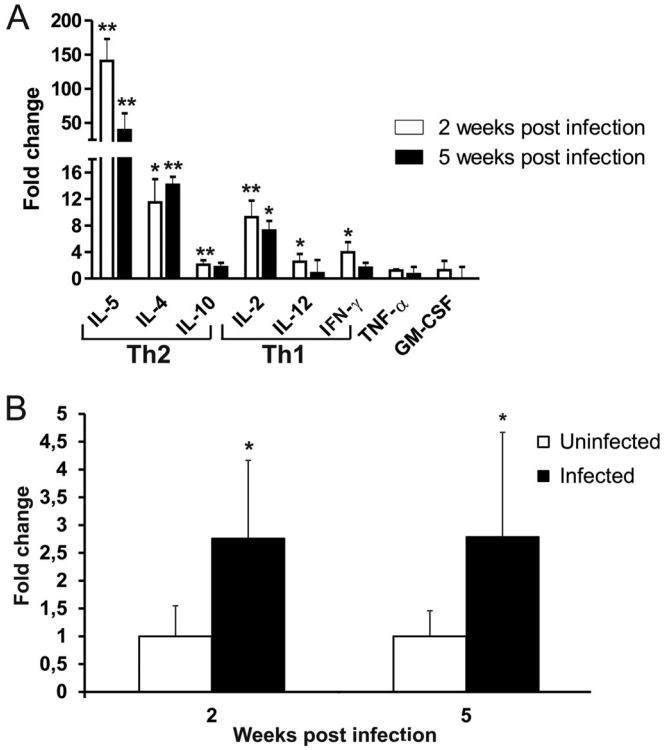

FIG 2 Predominant Th2 cytokine expression in LP-BM5-infected mice. (A) Production of Th2 cytokines (IL-5, IL-4, IL-10) and Th1 cytokines (IL-2, IL-12, IFN-γ) from splenocytes obtained from uninfected or LP-BM5-infected mice. Infected and uninfected mice were sacrificed at 2 or 5 weeks after infection, spleen cells were cultured, and supernatants were harvested at 72 h for assay for all cytokines. Cytokine assays were performed as described in Materials and Methods. Fold change was calculated for every infected mouse by dividing the concentration of the cytokine (expressed as picograms per milliliter) by the mean value for the corresponding cytokine from uninfected controls. Values represent the means ± SDs for 5 animals. *, $P < 0.05$ versus uninfected mice at the same time point; **, $P < 0.01$ versus uninfected mice at the same time point. (B) Expression of the IL-5 gene. The fold change with respect to the value for the uninfected controls was calculated using the $2^{-\Delta\Delta CT}$ method with normalization of the raw data to the data for the housekeeping gene GAPDH (glyceraldehyde-3-phosphate dehydrogenase). Data analysis was performed using web-based RT^2 Profiler PCR array data analysis software (SABiosciences). Values represent the means for 3 animals and were obtained at 2 and 5 weeks postinfection. The error bars represent 95% confidence intervals. *, $P < 0.05$ versus uninfected mice at the same time point.

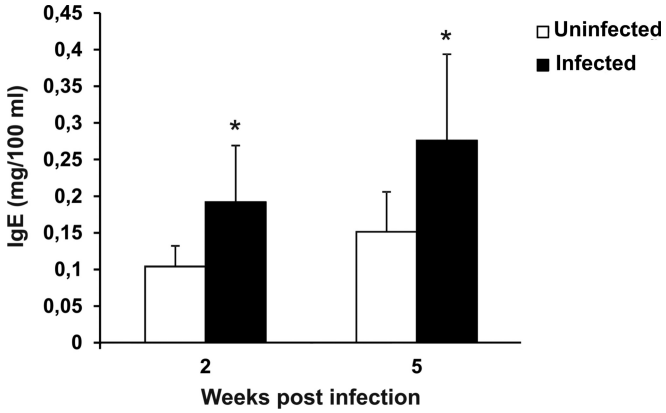

FIG 3 Increased IgE levels in LP-BM5-infected mice. The plasma IgE level in uninfected and infected mice was measured at 2 and 5 weeks after viral infection. Mouse infection and the methods used for determination of IgE levels are described in Materials and Methods. Values represent the means ± SDs for 5 animals. *, $P < 0.05$ versus uninfected mice at the same time point.

reported in Fig. 5 show that the LP-BM5 DNA copy numbers measured are proportional to the number of RT units of LP-BM5 RT used to infect the macrophages (Fig. 5, lower left). In macrophages infected with the low dose (0.5 RT unit), the GSH level was already significantly reduced at 6 days postinfection, while at the high dose (1 RT unit), both GSH and cysteine contents were significantly lower than those in uninfected macrophages at 3 and 6 days postinfection (Fig. 5, top). Moreover, IL-12 p40 mRNA levels were downregulated compared with those in uninfected macrophages, being significantly inhibited at 6 days postinfection in macrophages infected with the low dose (Fig. 5, lower right), while in macrophages infected with the high dose, IL-12 p40 mRNA was undetectable at either time point.

Effect of I-152 in LP-BM5-infected mice. A second *in vivo* experimental LP-BM5 infection was conducted to detect the immunomodulatory activity of the I-152 molecule. I-152 is a precursor of *N*-acetyl-cysteine (NAC) and beta-mercaptoethylamine (cysteamine) that is able to increase the *in vitro* intracellular GSH content and that has antiviral properties (36). The capacity of I-152 to increase thiol levels in the organs of LP-BM5-infected mice and to enhance the Th1 immune response was evaluated in the present study.

The antiviral effect of I-152 was previously demonstrated in the MAIDS model (37) and was confirmed in the present study, as revealed by reduced splenomegaly and lymphadenopathy; this effect was particularly evident at 9 weeks of treatment (Fig. 6).

The capacity of I-152 to restore the intracellular content of the thiol species in LP-BM5-infected mice was assessed by measuring GSH and cysteine levels in all organs, and the results obtained for the spleen and lymph nodes, which were those organs that underwent the most significant GSH/cysteine depletion, are reported in Fig. 7. We observed that I-152 treatment was able to reestablish the levels of GSH and cysteine in both the spleens and lymph nodes to the values in the spleens and lymph nodes of uninfected mice, while significant decreases in the amounts of both thiol species were confirmed in infected mice (data not shown). Only the results obtained at 2 weeks postinfection are shown in Fig. 7, since the results obtained at the following time points were comparable to those obtained at 2 weeks.

To investigate whether the restoration of GSH/cysteine levels through I-152 treatment could influence the amounts of Th1/Th2 cytokines from spleen cells of infected I-152-treated mice released into the culture medium, the expression of Th2 (IL-5, IL-4, IL-10) and Th1 (IL-2, IL-12, IFN-γ) cytokines was investigated at 2, 5, and 9 weeks after viral infection. Quantitative analysis revealed that at 2 weeks postinfection, the levels of IL-5 were significantly decreased; meanwhile, the amount of IFN-γ was significantly increased compared with that in infected and untreated animals (Fig. 8, white bars). At 5 weeks postinfection, the levels of IL-5 and IL-4 secreted by the spleens of infected and treated mice were significantly lower than those secreted by the spleens of infected mice (Fig. 8, black bars). Real-time PCR analysis of cDNA displayed a significant decrease in the levels of IL-5 transcripts from infected I-152-treated mice at 2 weeks postinfection (data not shown). The results obtained at 5 weeks postinfection were comparable to those obtained at 2 weeks (data not shown).

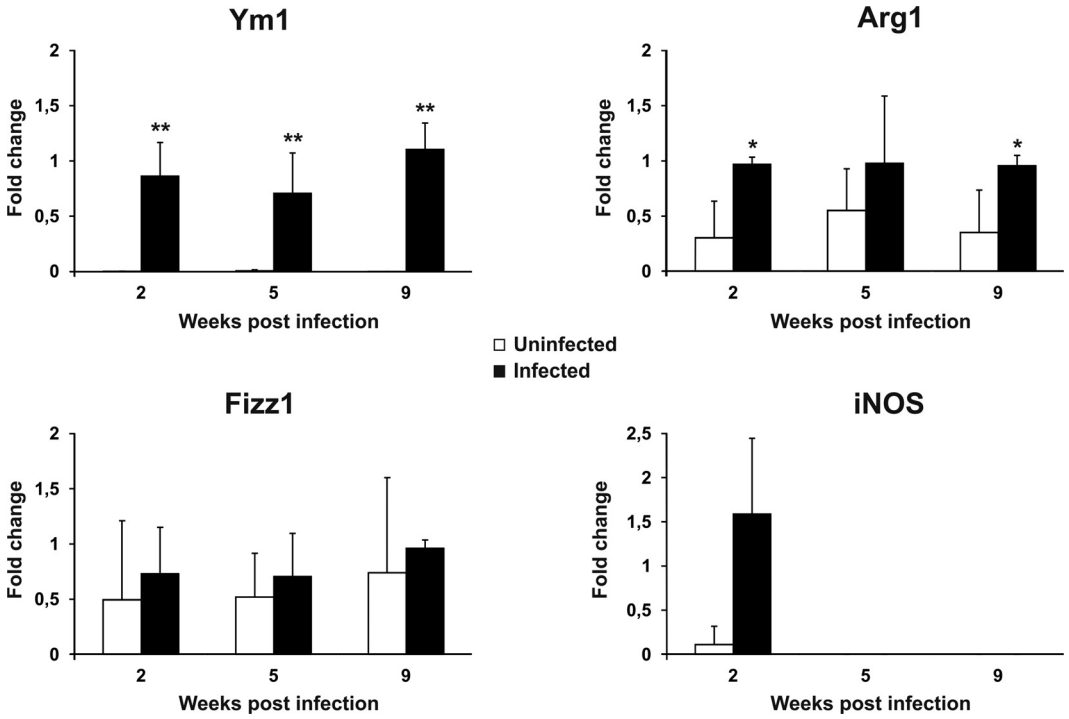

FIG 4 Alternative activation of macrophages in LP-BM5-infected mice. The levels of Ym1, Arg1, Fizz1, and iNOS mRNA in uninfected and infected mice were determined as reported in Materials and Methods. The β-actin gene was used as an internal reference. Relative quantification was performed by real-time RT-PCR according to the $2^{-\Delta\Delta CT}$ comparative method, and data are expressed as the mean fold change compared to the value for the calibrator sample (one infected mouse at each time after infection) ± SD for 5 animals. *, $P < 0.05$ versus uninfected mice at the same time point; **, $P < 0.01$ versus uninfected mice at the same time point.

I-152 treatment also influenced the activation status of peritoneal macrophages, reducing the levels of expression of AAMϕ markers in an apparent time-dependent fashion. In particular, although Arg1 and Fizz1 were already significantly downmodulated at 2 weeks postinfection, at 5 weeks postinfection both the infected and untreated mice and the infected and I-152-treated mice expressed similar levels of the same genes. On the other hand, a more pronounced effect of I-152 was seen at 9 weeks postinfection, not only because the amounts of Ym1, Arg1, and Fizz1 were decreased but also because, in two out of five mice analyzed, the expression of iNOS was induced 2-fold compared with the highest level observed in infected mice at 2 weeks postinfection (Fig. 9).

For all the parameters examined, the results obtained for infected mice treated with placebo were not different from those for infected untreated mice.

DISCUSSION

An alteration in the intracellular redox balance characterizes several viral infections and the progression of virus-induced diseases (52). It has been demonstrated that intracellular redox status alterations are often associated with the depletion of GSH (23–25). In this investigation, we found that important redox perturbations consisting of decreases in GSH and/or cysteine levels occur in the organs of LP-BM5 retrovirus-infected mice. In particular, spleen and lymph nodes, which are the organs containing the highest BM5d content and undergoing the most significant phenotypic as well as proliferative changes (11, 51), showed the most significant drops in GSH and/or cysteine levels. It will be interesting to learn more about the mechanism(s) by which this viral infection induces a decrease in the intracellular GSH content. In fact, in some cases, GSH depletion occurs at early time points after viral infection (53); in other cases, increased levels of inflammatory cytokines can induce GSH depletion, which, in turn, may activate redox-sensitive transcription factors, such as NF-κB, leading to downstream signal transduction events favoring viral expression (54). In the pancreas and brain, where the viral loads measured were significantly lower than those measured in the spleen and lymph nodes (data not shown), we found less dramatic decreases in the amounts of the thiol species analyzed. These data suggest that the extent of the decrease in GSH and cysteine levels could be linked to the viral load of the organ, and this hypothesis was demonstrated in *in vitro* experiments. Indeed, the results obtained from *in vitro* infection of macrophages showed that GSH depletion occurs at the very early stages of infection and depends on the viral load, suggesting that it may be a direct effect of the viral infection. However, this aspect requires deeper investigation.

Although the GSH perturbation in the pancreas and brain was not as important as that in the spleen and lymph nodes, the GSH perturbation observed in the pancreas and brain may have a role in the exocrine pancreatitis and encephalopathy characterizing LP-BM5 infection. In fact, the decrease in pancreatic cysteine levels may be due to the use of the amino acid for GSH synthesis, which would be necessary as a consequence of the upregulation of glutathione *S*-transferase previously described (55).

In brain, a significant decrease in the GSH level was measured after 5 weeks of infection. In MAIDS, spatial learning and memory deficits were described, although the brain viral titer has been

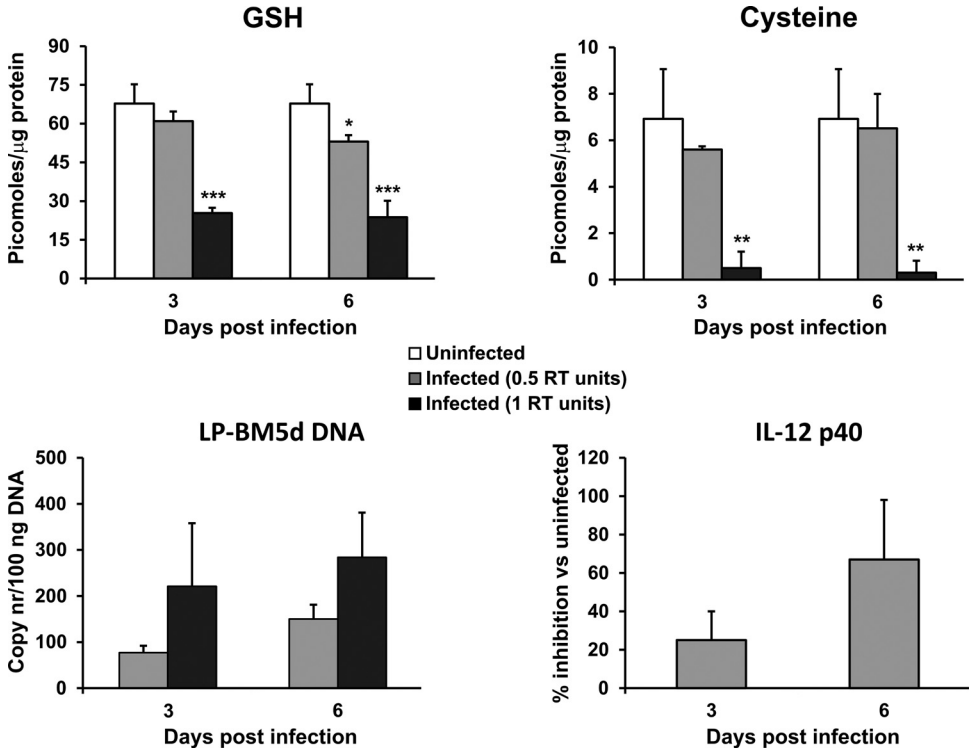

FIG 5 Decreased thiol content and inhibited expression of IL-12 p40 mRNA in macrophages infected with LP-BM5. The levels of GSH, cysteine, LP-BM5d DNA, and IL-12 p40 in murine peritoneal macrophages infected with 0.5 and 1 unit of RT were analyzed at 3 and 6 days postinfection. Infection of the macrophages and evaluation of the different parameters were performed as described in Materials and Methods. Values represent the means ± SDs for 3 samples. *, $P < 0.05$ versus uninfected mice at the same time point; **, $P < 0.01$ versus uninfected mice at the same time point; ***, $P < 0.005$ versus uninfected mice at the same time point. nr, number.

found to be very low (29–31, 51). Hence, it is not possible to establish whether the presence of the virus is responsible for the neuronal alterations observed (31). Actually, we could not establish the cause of the GSH depletion found, but we suggest that it may contribute to the neuronal alterations described in MAIDS, as has already been observed in other neurodegenerative disorders, such as Alzheimer's disease (56). This aspect is worth further investigation; in fact, it would be interesting to evaluate the capacity of GSH precursors able to cross the blood-brain barrier to diminish the encephalopathy that develops in these mice by replenishment of GSH levels (57). The finding that I-152 could increase GSH/cysteine levels in the brains of infected mice (not shown) is very interesting, and it will be the subject of future studies.

LP-BM5 infection can affect the balance of Th subset expression and promote the Th2 response (11–15), although C57BL/6 mice are predisposed toward the production of Th1 cytokines (58). In this investigation, a central role of Th2 cells in LP-BM5 infection was shown by using a multiplexed assay, which allowed us to detect all the cytokines in the supernatants of unstimulated spleen cells at every time point examined, including those present at lower concentrations (59, 60). The results, corroborated by cytokine expression analysis through PCR array analysis, showed that the infection was characterized by two main phases distin-

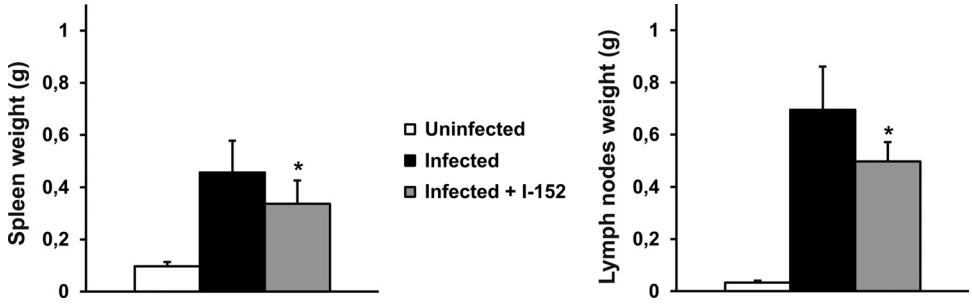

FIG 6 Inhibition of splenomegaly and lymphadenopathy in LP-BM5-infected mice treated with I-152. Mice were infected as described in Materials and Methods and treated i.p. with I-152 (30 μmol/mouse) 3 days a week for a total of 9 weeks. Values represent the means ± SDs for 5 animals and were obtained at 9 weeks postinfection. *, $P < 0.05$.

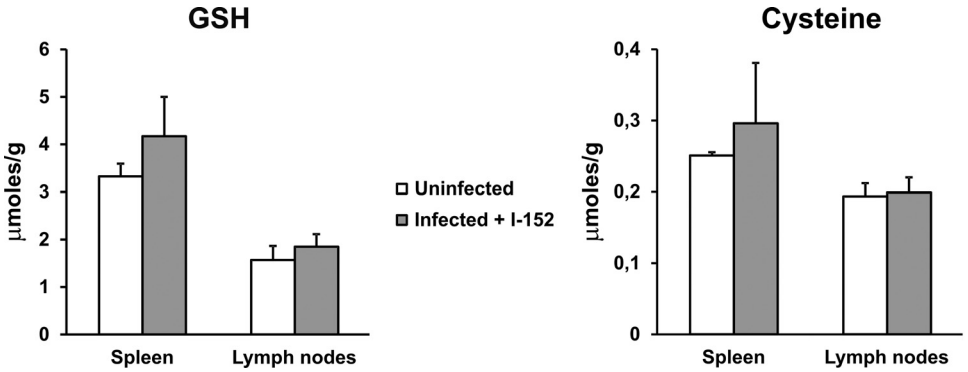

FIG 7 Increased GSH and cysteine levels in spleen and lymph nodes of LP-BM5-infected mice treated with I-152. Mice were infected as described in Materials and Methods and treated i.p. with I-152 (30 μmol/mouse) 3 days a week for a total of 9 weeks. GSH and cysteine levels were determined by the procedure described in Materials and Methods. Results refer to those obtained at 2 weeks postinfection. Values represent the means ± SDs for 5 animals.

guished by different cytokine profiles. During the first 2 weeks, LP-BM5 viral infection induced a $CD4^+$ T-cell response characterized by the expression of Th1 and Th2 cytokines, with a prevalence of Th2 cytokines, as revealed by high levels of IL-5 and IL-4. The progression of viral infection (at 5 or 9 weeks postinfection) was characterized by a general decrease in cytokine production, although the prevalence of Th2 cytokines persisted; in fact, IL-4 and IL-5 were still present at very high concentrations ($P < 0.01$), while IL-12 as well as IFN-γ returned to control levels, and IL-2 was the only Th1 cytokine still present at a significantly higher concentration than the other Th1 cytokines ($P < 0.05$).

The prevalent Th2 response was also supported by IgE production, which is the most distinctive effect of IL-4 *in vivo* (61), although IgE switching in LP-BM5-infected mice could also be regulated by IL-4-independent pathways (12, 13). The preferential activation of Th2-type cells has been accounted for by the important role of B cells in *in vivo* T-cell activation in this infection, where antigen presentation by B cells favors the activation of Th2 clones (11, 62, 63). The results reported herein provide further insight into the role that GSH and macrophages could have in disease progression and Th1/Th2 cytokine production during LP-BM5 infection. In fact, as already observed, low levels of GSH were measured in all organs examined and, in particular, in spleen and lymph nodes. At 2 weeks postinfection, when both Th1 and Th2 responses were present with a higher prevalence of the latter, GSH depletion was not observed, but reduced cysteine levels in spleen and lymph nodes were measured, and these were statistically significantly reduced in the spleen. Diminished cysteine levels may be a consequence of the use of this amino acid in GSH synthesis. At this time point, viral replication is low and cysteine stores may be sufficient to replenish normal GSH levels. Indeed, a correlation between redox alteration and LP-BM5 infection in the very early phases of infection is supported by *in vitro* studies conducted with macrophages, where the extent of the decreases in GSH and cysteine levels depended on the infecting dose and reduced IL-12 p40

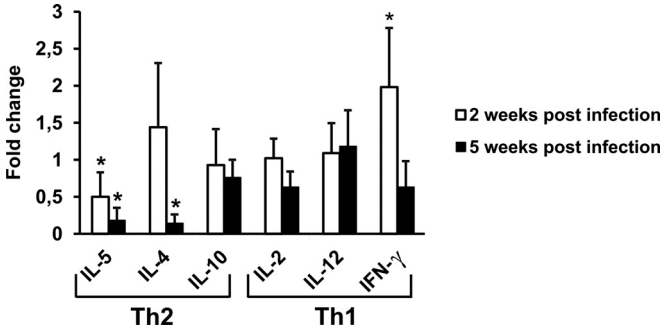

FIG 8 Inhibition of Th2 cytokine expression in LP-BM5-infected mice treated with I-152. The levels of production of Th1 cytokines (IL-2, IL-12, IFN-γ) and Th2 cytokines (IL-5, IL-4, IL-10) from splenocytes obtained from infected mice that were untreated or treated with I-152 were determined. Mice were infected as reported in Materials and Methods, spleen cells were cultured at 2 and 5 weeks after infection, and supernatants were harvested at 72 h of culture for assays of all cytokines. Cytokine assays were performed as described in Materials and Methods. Fold change was calculated for every infected I-152-treated mouse by dividing the concentration of the cytokine (expressed in picograms per milliliter) by the mean value for the corresponding cytokine for infected mice. Values represent the means ± SDs for 5 animals. *, $P < 0.05$ versus infected mice at the same time point.

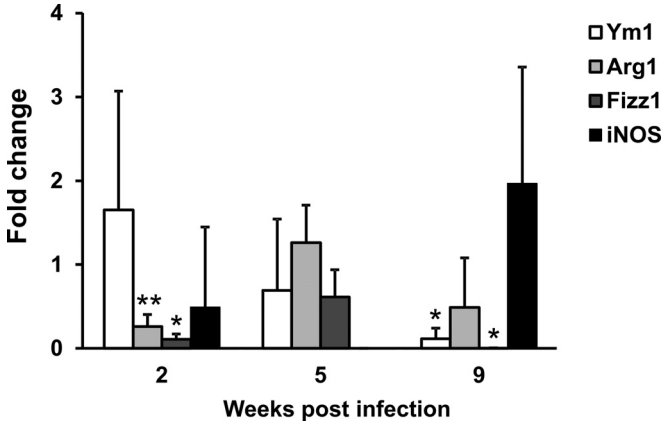

FIG 9 Inhibition of AAMϕ marker genes by I-152. The levels of Ym1, Arg1, Fizz1, and iNOS mRNA in infected I-152-treated mice compared with those in infected mice were determined. β-Actin was used as an internal reference gene. Relative quantification was performed by real-time RT-PCR according to the $2^{-\Delta\Delta CT}$ comparative method, and data are expressed as the mean fold change compared to the value for the calibrator sample (one infected mouse at each time after infection) ± SD for 5 animals. *, $P < 0.05$ versus infected mice at the same time point; **, $P < 0.01$ versus infected mice at the same time point. The expression of iNOS at 9 weeks was calibrated to the value for infected mice at 2 weeks. Because iNOS was expressed in only two out of five mice, statistical analysis was not performed.

mRNA levels were expressed. These results are in agreement with those of previous studies showing that a decreased intracellular GSH content is linked to reduced levels of IL-12 secretion and to skewing toward a Th2 response (17, 18).

It is interesting to note that at 5 or 9 weeks postinfection, when significantly higher levels of Th2 cytokines, i.e., IL-4 and IL-5, than other cytokines were still present, an altered redox state was found.

A strict correlation between the GSH content and the Th response in LP-BM5 infection was finally demonstrated when LP-BM5-infected mice were treated with I-152, a precursor of NAC and cysteamine, which can be used for GSH synthesis. The antiviral effect of I-152 against HIV-1 was assessed *in vitro* (36). Moreover, we have previously demonstrated that daily treatment with I-152 at a concentration, in molar equivalents, about 10 times lower than that of GSH moderated the development of MAIDS symptoms and the amount of BM5d proviral DNA in lymphoid organs (37). In the present work, I-152, which was administered three times a week instead of daily, was able to restore GSH and cysteine levels in all the organs examined, including spleen and lymph nodes. Despite the use of doses of I-152 lower than those used previously (37), the treatment was still able to reduce the signs of the disease, i.e., splenomegaly and lymphadenopathy. Moreover, at 2 weeks postinfection, I-152 administration favored the production of IFN-γ and inhibited the production of IL-5, while at 5 weeks postinfection, a significant inhibition of the Th2 immune response, as revealed by the low concentrations of IL-4 and IL-5, was observed. Consistent with the well-known reciprocal relationship between the production of IFN-γ and IL-4 (64), the increase in IFN-γ levels by splenocytes from infected I-152-treated mice was accompanied by decreased IL-4 levels in splenocytes from such mice. Hence, in agreement with previous *in vitro* and *in vivo* works showing that GSH levels influence IL-12 production and Th response patterns (17, 18, 38, 39), we can conclude that in MAIDS Th1/Th2 cytokines can also be influenced by the redox state. Moreover, the molecules able to increase the intracellular GSH content can favor and inhibit Th1 and Th2 cytokines, respectively, thus reestablishing a Th1/Th2 balance.

In agreement with a prevalent Th2 immune response, we demonstrated that LP-BM5 infection was characterized by the recruitment of AAMϕ at every time point studied. The expression of genes coding for Fizz1, Arg1, and Ym1 was always induced. In contrast, expression of iNOS, which is a marker of classical activation of macrophages, was detected at the early stages of infection (2 weeks), when Th1 cytokines were expressed at higher levels than at other times investigated, and in only about 50% of animals. These results are in agreement with those of other studies showing a correlation between a Th2 cytokine environment and high levels of expression of Fizz1 and/or Ym1 in peritoneal macrophages (33, 34). Hence, we have clearly established the phenotype of AAMϕ during LP-BM5 infection, but the exact function of these cells has yet to be characterized. It has to be considered that this study analyzed *in vivo* the net outcome of even small changes from a wide variety of cell types. Also, M1 and M2 macrophages are not strictly separable clones like Th1 and Th2. Rather, they can present with a full array of phenotypes between the two most extreme. In this context, it is the propensity of the whole environment that determines the overall response of the organism (65). It is known that AAMϕ produce low levels of IL-12 (32), contributing to the switch between Th1 and Th2 responses in several diseases (21–23, 66). On the other hand, it is possible to regulate the amount of IL-12 secreted by increasing the intracellular GSH levels, and an IL-12^{low} macrophage phenotype could be changed into an IL-12^{high} macrophage phenotype (67). In agreement with an inhibited Th2 immune response and, in particular, with reduced IL-4 levels through I-152 treatment, the expression of genes characterizing AAMϕ was found to be reduced. In addition, at 9 weeks

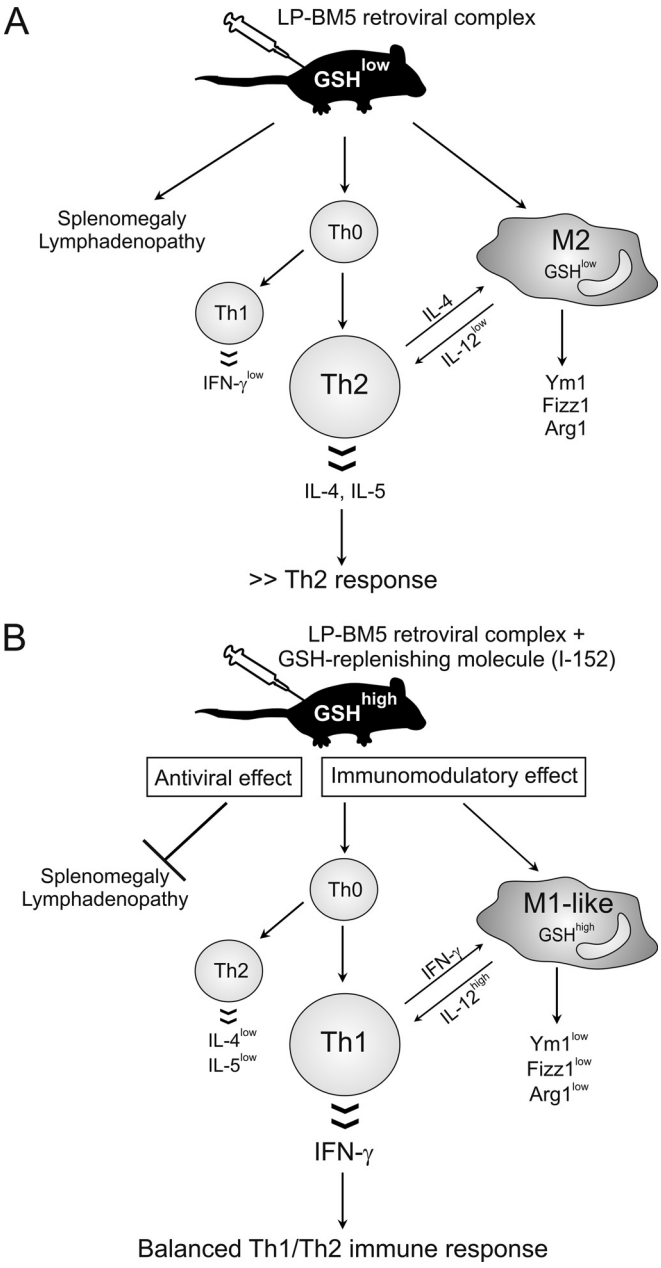

FIG 10 Inhibition of MAIDS by GSH-replenishing molecules. (A) LP-BM5 infection is characterized by several immune dysfunctions, including splenomegaly and lymphadenopathy (1–4), and GSH deficiency, which favors a Th2 immune response as well as an alternatively activated macrophage phenotype, distinguished by the expression of the genetic markers Fizz1, Ym1, and Arg1. (B) The inhibitory effect of I-152 on MAIDS can be considered the result of two mechanisms of action: on the one hand, it can directly hamper viral replication; on the other hand, it can inhibit and stimulate Th2 and Th1 cytokine production, respectively, reestablishing a balanced Th1/Th2 immune response.

postinfection, the expression of the M1 gene iNOS was found to be increased, suggesting that the switch from M2- to M1-like macrophages could be a slower mechanism sustained by the Th2-to-Th1 switch. In fact, IL-4 can act as a stimulus to drive the expression of many M2 markers (34, 68), and the data presented here show that I-152 could be used to change the M2 macrophage phenotype. It would be interesting, given the results of the effect of I-152 treatment on peritoneal macrophages obtained here, to test the activity of the molecule against other cells of the myeloid lineage in the context of LP-BM5 retrovirus-induced disease. Specifically, recent reports have detailed augmented monocytic myeloid-derived suppressor cell (M-MDSC) production during LP-BM5-induced disease, including immunodeficiency (69–72). Because the mechanism of inhibition of T-cell responses by these M-MDSCs for inhibition of T-cell responses was fully dependent on iNOS/NO, whereas iNOS/NO was responsible for about 50% of the inhibition of B-cell responses, it would be interesting to study I-152 treatment to determine whether M-MDSC numbers and suppressive activity can be increased or decreased in LP-BM5-infected mice. The present study shows that in LP-BM5 infection, GSH depletion and AAMϕ could have an important role in determining the Th2 immune response and that I-152 treatment may represent a useful approach to fight this retroviral infection (Fig. 10). The main advantage of using I-152 and, presumably, other GSH-replenishing molecules derives from their dual mechanisms of action: on the one hand, they can directly inhibit viral replication; on the other hand, they can reestablish a correct GSH content in antigen-presenting cells favoring the production of cytokines which induce the Th1 immune response. In conclusion, GSH-replenishing molecules could be considered new tools that act as both immunomodulators and antivirals.

ACKNOWLEDGMENTS

We thank Timothy C. Bloom for his linguistic revision of the article and Davide Sisti for his advice on statistics.

FUNDING INFORMATION

This work, including the efforts of Alessandra Fraternale, was funded by Ministero dell'Istruzione, dell'Università e della Ricerca (MIUR) (PRIN [Research Projects of National Interest] 2010-2011-prot. 2010PHT9NF_004).

REFERENCES

1. **Mosier DE.** 1986. Animal models for retrovirus-induced immunodeficiency disease. Immunol Invest **15:**233–261. http://dx.doi.org/10.3109/08820138609026687.
2. **Mosier DE, Yetter RA, Morse HC, III.** 1985. Retroviral induction of acute lymphoproliferative disease and profound immunosuppression in adult C57BL/6 mice. J Exp Med **161:**766–784. http://dx.doi.org/10.1084/jem.161.4.766.
3. **Hartley JW, Fredrickson TN, Hartley JW, Yetter RA, Morse HC, III.** 1989. Retrovirus-induced murine acquired immunodeficiency syndrome: natural history of infection and differing susceptibility of inbred mouse strains. J Virol **63:**1223–1231.
4. **Klinken SP, Fredrickson TN, Hartley JW, Yetter RA, Morse HC, III.** 1988. Evolution of B cell lineage lymphomas in mice with a retrovirus-induced immunodeficiency syndrome, MAIDS. J Immunol **140:**1123–1131.
5. **Cao L, Butler MB, Tan L, Draleau KS, Koh WY.** 2012. Murine immunodeficiency virus-induced peripheral neuropathy and associated cytokine responses. J Immunol **189:**3724–3733. http://dx.doi.org/10.4049/jimmunol.1201313.
6. **Dias AS, Bester MJ, Britz RF, Apostolides Z.** 2006. Animal models used for the evaluation of antiretroviral therapies. Curr HIV Res **4:**431–446. http://dx.doi.org/10.2174/157016206778560045.
7. **Eiseman JL, Yetter RA, Fredrickson TN, Shapiro SG, MacAuley C, Bilello JA.** 1991. Effect of 3′azidothymidine administered in drinking water or by continuous infusion on the development of MAIDS. Antiviral Res **16:**307–326. http://dx.doi.org/10.1016/0166-3542(91)90046-T.
8. **Palamara AT, Garaci E, Rotilio G, Ciriolo MR, Casabianca A, Fraternale A, Rossi L, Schiavano GF, Chiarantini L, Magnani M.** 1996. Inhibition of murine AIDS by reduced glutathione. AIDS Res Hum Retroviruses **12:**1373–1381. http://dx.doi.org/10.1089/aid.1996.12.1373.
9. **Fraternale A, Casabianca A, Tonelli A, Vallanti G, Chiarantini L, Brandi G, Celeste AG, Magnani M.** 2000. Inhibition of murine AIDS by alternate administration of azidothymidine and fludarabine monophosphate. J Acquir Immune Defic Syndr **23:**209–220.
10. **Fraternale A, Casabianca A, Tonelli A, Chiarantini L, Brandi G, Magnani M.** 2001. New drug combinations for the treatment of murine AIDS and macrophage protection. Eur J Clin Invest **31:**248–252. http://dx.doi.org/10.1046/j.1365-2362.2001.00806.x.
11. **Gazzinelli RT, Makino M, Chattopadhyay SK, Snapper CM, Sher A, Hügin AW, Morse HC, III.** 1992. $CD4^+$ subset regulation in viral infection. Preferential activation of Th2 cells during progression of retrovirus-induced immunodeficiency in mice. J Immunol **148:**182–188.
12. **Morawetz RA, Gabriele L, Rizzo LV, Noben-Trauth N, Kühn R, Rajewsky K, Müller W, Doherty TM, Finkelman F, Coffman RL, Morse HC, III.** 1996. Interleukin (IL)-4-independent immunoglobulin class switch to immunoglobulin (Ig)E in the mouse. J Exp Med **184:**1651–1661. http://dx.doi.org/10.1084/jem.184.5.1651.
13. **Morse HC, III, McCarty T, Giese NA, Taddesse-Heath L, Grusby MJ.** 1999. STAT6-deficient mice exhibit normal induction of murine AIDS and expression of immunoglobulin E following infection with LP-BM5 murine leukemia viruses. J Virol **73:**7093–7095.
14. **Morawetz RA, Doherty TM, Giese NA, Hartley JW, Müller W, Kühn R, Rajewsky K, Coffman R, Morse HC, III.** 1994. Resistance to murine acquired immunodeficiency syndrome (MAIDS). Science **265:**264–266.
15. **Sher A, Gazzinelli RT, Oswald IP, Clerici M, Kullberg M, Pearce EJ, Berzofsky JA, Mosmann TR, James SL, Morse HC, III.** 1992. Role of T-cell derived cytokines in the downregulation of immune responses in parasitic and retroviral infection. Immunol Rev **127:**183–204. http://dx.doi.org/10.1111/j.1600-065X.1992.tb01414.x.
16. **Desmedt M, Rotiers P, Dooms H, Fiers W, Grooten J.** 1998. Macrophages induce cellular immunity by activating Th1 cell responses and suppressing Th2 cell responses. J Immunol **160:**5300–5308.
17. **Dobashi K, Aihara M, Araki T, Shimizu Y, Utsugi M, Iizuka K, Murata Y, Hamuro J, Nakazawa T, Mori M.** 2001. Regulation of LPS induced IL-12 production by IFN-γ and IL-4 through intracellular glutathione status in human alveolar macrophages. Clin Exp Immunol **124:**290–296. http://dx.doi.org/10.1046/j.1365-2249.2001.01535.x.
18. **Peterson JD, Herzenberg LA, Vasquez K, Waltenbaugh C.** 1998. Glutathione levels in antigen-presenting cells modulate Th1 versus Th2 response patterns. Proc Natl Acad Sci U S A **95:**3071–3076. http://dx.doi.org/10.1073/pnas.95.6.3071.
19. **Romagnani S.** 2000. T-cell subsets (Th1 versus Th2). Ann Allergy Asthma Immunol **85:**9–18. http://dx.doi.org/10.1016/S1081-1206(10)62426-X.
20. **Becker Y.** 2004. The changes in the T helper 1 (Th1) and T helper 2 (Th2) cytokine balance during HIV-1 infection are indicative of an allergic response to viral proteins that may be reversed by Th2 cytokine inhibitors and immune response modifiers—a review and hypothesis. Virus Genes **28:**5–18. http://dx.doi.org/10.1023/B:VIRU.0000012260.32578.72.
21. **Dwivedi VP, Bhattacharya D, Chatterjee S, Prasad DV, Chattopadhyay D, Van Kaer L, Bishai WR, Das G.** 2012. Mycobacterium tuberculosis directs T helper 2 cell differentiation by inducing interleukin-1β production in dendritic cells. J Biol Chem **287:**33656–33663. http://dx.doi.org/10.1074/jbc.M112.375154.
22. **Piedrafita D, Proudfoot L, Nikolaev AV, Xu D, Sands W, Feng GJ, Thomas E, Brewer J, Ferguson MA, Alexander J, Liew FY.** 1999. Regulation of macrophage IL-12 synthesis by Leishmania phosphoglycans. Eur J Immunol **29:**235–244.
23. **Venketaraman V, Millman A, Salman M, Swaminathan S, Goetz M, Lardizabal A, Hom D, Connell ND.** 2008. Glutathione levels and immune responses in tuberculosis patients. Microb Pathog **44:**255–261. http://dx.doi.org/10.1016/j.micpath.2007.09.002.
24. **Helbling B, von Overbeck J, Lauterburg BH.** 1996. Decreased release of glutathione into the systemic circulation of patients with HIV infection.

Eur J Clin Invest **26:**38–44. http://dx.doi.org/10.1046/j.1365-2362.1996.88237.x.

25. **Morris D, Ly J, Chi PT, Daliva J, Nguyen T, Soofer C, Chen YC, Lagman M, Venketaraman V.** 2014. Glutathione synthesis is compromised in erythrocytes from individuals with HIV. Front Pharmacol **5:**73. http://dx.doi.org/10.3389/fphar.2014.00073.
26. **Herzenberg LA, De Rosa SC, Dubs JG, Roederer M, Anderson MT, Ela SW, Deresinski SC, Herzenberg LA.** 1997. Glutathione deficiency is associated with impaired survival in HIV disease. Proc Natl Acad Sci U S A **94:**1967–1972. http://dx.doi.org/10.1073/pnas.94.5.1967.
27. **Yetter RA, Buller RM, Lee JS, Elkins KL, Mosier DE, Fredrickson TN, Morse HC, III.** 1988. $CD4^+$ T cells are required for development of a murine retrovirus-induced immunodeficiency syndrome (MAIDS). J Exp Med **168:**623–635. http://dx.doi.org/10.1084/jem.168.2.623.
28. **Kawauchi Y1, Suzuki K, Watanabe S, Yamagiwa S, Yoneyama H, Han GD, Palaniyandi SS, Veeraveedu PT, Watanabe K, Kawachi H, Okada Y, Shimizu F, Asakura H, Aoyagi Y, Narumi S.** 2006. Role of IP-10/CXCL10 in the progression of pancreatitis-like injury in mice after murine retroviral infection. Am J Physiol Gastrointest Liver Physiol **291:**G345–G354. http://dx.doi.org/10.1152/ajpgi.00002.2006.
29. **Kustova Y, Espey MG, Sung EG, Morse D, Sei Y, Basile AS.** 1998. Evidence of neuronal degeneration in C57B1/6 mice infected with the LP-BM5 leukemia retrovirus mixture. Mol Chem Neuropathol **35:**39–59. http://dx.doi.org/10.1007/BF02815115.
30. **Sei Y, Arora PK, Skolnick P, Paul IA.** 1992. Spatial learning impairment in a murine model of AIDS. FASEB J **6:**3008–3013.
31. **Sei Y, Kustova Y, Li Y, Morse HC, III, Skolnick P, Basile AS.** 1998. The encephalopathy associated with murine acquired immunodeficiency syndrome. Ann N Y Acad Sci **840:**822–834. http://dx.doi.org/10.1111/j.1749-6632.1998.tb09620.x.
32. **Fraternale A, Brundu S, Magnani M.** 2015. Polarization and repolarization of macrophages. J Clin Cell Immunol **6:**319.
33. **Donnelly S, O'Neill SM, Sekiya M, Mulcahy G, Dalton JP.** 2005. Thioredoxin peroxidase secreted by Fasciola hepatica induces the alternative activation of macrophages. Infect Immun **73:**166–173. http://dx.doi.org/10.1128/IAI.73.1.166-173.2005.
34. **Raes G, De Baetselier P, Noël W, Beschin A, Brombacher F, Hassanzadeh Gh G.** 2002. Differential expression of FIZZ1 and Ym1 in alternatively versus classically activated macrophages. J Leukoc Biol **71:**597–602.
35. **Chang NC, Hung SI, Hwa KY, Kato I, Chen JE, Liu CH, Chang AC.** 2001. A macrophage protein, Ym1, transiently expressed during inflammation is a novel mammalian lectin. J Biol Chem **276:**17497–17506. http://dx.doi.org/10.1074/jbc.M010417200.
36. **Oiry J, Mialocq P, Puy JY, Fretier P, Dereuddre-Bosquet N, Dormont D, Imbach JL, Clayette P.** 2004. Synthesis and biological evaluation in human monocyte-derived macrophages of *N*-(*N*-acetyl-L-cysteinyl)-*S*-acetylcysteamine analogues with potent antioxidant and anti-HIV activities. J Med Chem **47:**1789–1795. http://dx.doi.org/10.1021/jm030374d.
37. **Fraternale A, Paoletti MF, Casabianca A, Orlandi C, Schiavano GF, Chiarantini L, Clayette P, Oiry J, Vogel J-U, Cinatl J, Jr, Magnani M.** 2008. Inhibition of murine AIDS by pro-glutathione (GSH) molecules. Antiviral Res **77:**120–127. http://dx.doi.org/10.1016/j.antiviral.2007.11.004.
38. **Fraternale A, Paoletti MF, Dominici S, Caputo A, Castaldello A, Millo E, Brocca-Cofano E, Smietana M, Clayette P, Oiry J, Benatti U, Magnani M.** 2010. The increase in intra-macrophage thiols induced by new pro-GSH molecules directs the Th1 skewing in ovalbumin immunized mice. Vaccine **28:**7676–7682. http://dx.doi.org/10.1016/j.vaccine.2010.09.033.
39. **Fraternale A, Paoletti MF, Dominici S, Buondelmonte C, Caputo A, Castaldello A, Tripiciano A, Cafaro A, Palamara AT, Sgarbanti R, Garaci E, Ensoli B, Magnani M.** 2011. Modulation of Th1/Th2 immune responses to HIV-1 Tat by new pro-GSH molecules. Vaccine **29:**6823–6829. http://dx.doi.org/10.1016/j.vaccine.2011.07.101.
40. **Nucci C, Palamara AT, Ciriolo MR, Nencioni L, Savini P, D'Agostini C, Rotilio G, Cerulli L, Garaci E.** 2000. Imbalance in corneal redox state during herpes simplex virus 1-induced keratitis in rabbits. Effectiveness of exogenous glutathione supply. Exp Eye Res **70:**215–220.
41. **Buhl R, Jaffe HA, Holroyd KJ, Wells FB, Mastrangeli A, Saltini C, Cantin AM, Crystal RG.** 1989. Systemic glutathione deficiency in symptom-free HIV-seropositive individuals. Lancet **ii:**1294–1298.
42. **Ciriolo MR, Palamara AT, Incerpi S, Lafavia E, Buè MC, De Vito P, Garaci E, Rotilio G.** 1997. Loss of GSH, oxidative stress, and decrease of intracellular pH as sequential steps in viral infection. J Biol Chem **272:**2700–2708. http://dx.doi.org/10.1074/jbc.272.5.2700.
43. **Price TO, Ercal N, Nakaoke R, Banks WA.** 2005. HIV-1 viral proteins gp120 and Tat induce oxidative stress in brain endothelial cells. Brain Res **1045:**57–63. http://dx.doi.org/10.1016/j.brainres.2005.03.031.
44. **Okuda M, Li K, Beard MR, Showalter LA, Scholle F, Lemon SM, Weinman SA.** 2002. Mitochondrial injury, oxidative stress, and antioxidant gene expression are induced by hepatitis C virus core protein. Gastroenterology **122:**366–375. http://dx.doi.org/10.1053/gast.2002.30983.
45. **National Research Council.** 2011. Guide for the care and use of laboratory animals, 8th ed. National Academies Press, Washington, DC.
46. **Brundu S, Nencioni L, Celestino I, Coluccio P, Palamara AT, Magnani M, Fraternale A.** 2016. Validation of a reversed-phase high performance liquid chromatography method for the simultaneous analysis of cysteine and reduced glutathione in mouse organs. Oxid Med Cell Longev **2016:**1746985. http://dx.doi.org/10.1155/2016/1746985.
47. **Fraternale A, Crinelli R, Casabianca A, Paoletti MF, Orlandi C, Carloni E, Smietana M, Palamara AT, Magnani M.** 2013. Molecules altering the intracellular thiol content modulate NF-κB and STAT-1/IRF-1 signalling pathways and IL-12 p40 and IL-27 p28 production in murine macrophages. PLoS One **8:**e57866. http://dx.doi.org/10.1371/journal.pone.0057866.
48. **Fiorani M, De Sanctis R, Menghinello P, Cucchiarini L, Cellini B, Dachà M.** 2001. Quercetin prevents glutathione depletion induced by dehydroascorbic acid in rabbit red blood cells. Free Radic Res **34:**639–648. http://dx.doi.org/10.1080/10715760100300531.
49. **Sambrook J, Fritsch EF, Maniatis T.** 1989. Molecular cloning: a laboratory manual, p E3–E4, 2nd ed, vol 3. Cold Spring Harbor Laboratory Press, Cold Spring Harbor, NY.
50. **Pfaffl MW.** 2001. A new mathematical model for relative quantification in real-time RT-PCR. Nucleic Acids Res **29:**e45. http://dx.doi.org/10.1093/nar/29.9.e45.
51. **Casabianca A, Orlandi C, Fraternale A, Magnani M.** 2004. Development of a real-time PCR assay using SYBR green I for provirus load quantification in a murine model of AIDS. J Clin Microbiol **42:**4361–4364. http://dx.doi.org/10.1128/JCM.42.9.4361-4364.2004.
52. **Beck MA, Handy J, Levander OA.** 2000. The role of oxidative stress in viral infections. Ann N Y Acad Sci **917:**906–912.
53. **Palamara AT, Perno CF, Ciriolo MR, Dini L, Balestra E, D'Agostini C, Di Francesco P, Favalli C, Rotilio G, Garaci E.** 1995. Evidence for antiviral activity of glutathione: in vitro inhibition of herpes simplex virus type 1 replication. Antiviral Res **27:**237–253. http://dx.doi.org/10.1016/0166-3542(95)00008-A.
54. **Staal FJ, Roederer M, Herzenberg LA, Herzenberg LA.** 1990. Intracellular thiols regulate activation of nuclear factor kappa B and transcription of human immunodeficiency virus. Proc Natl Acad Sci U S A **87:**9943–9947. http://dx.doi.org/10.1073/pnas.87.24.9943.
55. **Löhr JM, Faissner R, Koczan D, Bewerunge P, Bassi C, Brors B, Eils R, Frulloni L, Funk A, Halangk W, Jesenofsky R, Kaderali L, Kleeff J, Krüger B, Lerch MM, Lösel R, Magnani M, Neumaier M, Nittka S, Sahin-Tóth M, Sänger J, Serafini S, Schnölzer M, Thierse HJ, Wandschneider S, Zamboni G, Klöppel G.** 2010. Autoantibodies against the exocrine pancreas in autoimmune pancreatitis: gene and protein expression profiling and immunoassays identify pancreatic enzymes as a major target of the inflammatory process. Am J Gastroenterol **105:**2060–2071. http://dx.doi.org/10.1038/ajg.2010.141.
56. **Saharan S, Mandal PK.** 2014. The emerging role of glutathione in Alzheimer's disease. J Alzheimers Dis **40:**519–529. http://dx.doi.org/10.3233/JAD-132483.
57. **Zeevalk GD, Manzino L, Sonsalla PK, Bernard LP.** 2007. Characterization of intracellular elevation of glutathione (GSH) with glutathione monoethyl ester and GSH in brain and neuronal cultures: relevance to Parkinson's disease. Exp Neurol **203:**512–520. http://dx.doi.org/10.1016/j.expneurol.2006.09.004.
58. **O'Garra A, McEvoy LM, Zlotnik A.** 1998. T-cell subsets: chemokine receptors guide the way. Curr Biol **8:**R646–R649. http://dx.doi.org/10.1016/S0960-9822(07)00413-7.
59. **Fu Q, Schoenhoff FS, Savage WJ, Zhang P, Van Eyk JE.** 2010. Multiplex assays for biomarker research and clinical application: translational science coming of age. Proteomics Clin Appl **4:**271–284. http://dx.doi.org/10.1002/prca.200900217.
60. **Prabhakar U, Eirikis E, Reddy M, Silvestro E, Spitz S, Pendley C, II, Davis HM, Miller BE.** 2004. Validation and comparative analysis of a

multiplexed assay for the simultaneous quantitative measurement of Th1/Th2 cytokines in human serum and human peripheral blood mononuclear cell culture supernatants. J Immunol Methods **291:**27–38. http://dx.doi.org/10.1016/j.jim.2004.04.018.
61. **Chatila TA.** 2004. Interleukin-4 receptor signaling pathways in asthma pathogenesis. Trends Mol Med **10:**493–499. http://dx.doi.org/10.1016/j.molmed.2004.08.004.
62. **Cerny A, Hügin AW, Hardy RR, Hayakawa K, Zinkernagel RM, Makino M, Morse HC, III.** 1990. B cells are required for induction of T cell abnormalities in a murine retrovirus-induced immunodeficiency syndrome. J Exp Med **171:**315–320. http://dx.doi.org/10.1084/jem.171.1.315.
63. **Gajewski TF, Pinnas M, Wong T, Fitch FW.** 1991. Murine Th1 and Th2 clones proliferate optimally in response to distinct antigen-presenting cell populations. J Immunol **46:**1750–1758.
64. **Farrar JD, Asnagli H, Murphy KM.** 2002. T helper subset development: roles of instruction, selection, and transcription. J Clin Invest **109:**431–435. http://dx.doi.org/10.1172/JCI0215093.
65. **Mills CD, Kincaid K, Alt JM, Heilman MJ, Hill AM.** 2000. M-1/M-2 macrophages and the Th1/Th2 paradigm. J Immunol **164:**6166–6173. http://dx.doi.org/10.4049/jimmunol.164.12.6166.
66. **Hamza T, Barnett JB, Li B.** 2010. Interleukin 12 a key immunoregulatory cytokine in infection applications. Int J Mol Sci **11:**789–806. http://dx.doi.org/10.3390/ijms11030789.
67. **Koike Y, Hisada T, Utsugi M, Ishizuka T, Shimizu Y, Ono A, Murata Y, Hamuro J, Mori M, Dobashi K.** 2007. Glutathione redox regulates airway hyperresponsiveness and airway inflammation in mice. Am J Respir Cell Mol Biol **37:**322–329. http://dx.doi.org/10.1165/rcmb.2006-0423OC.
68. **Nelson SM, Lei X, Prabhu KS.** 2011. Selenium levels affect the IL-4-induced expression of alternative activation markers in murine macrophages. J Nutr **141:**1754–1761. http://dx.doi.org/10.3945/jn.111.141176.
69. **Green KA, Cook WJ, Green WR.** 2013. Myeloid-derived suppressor cells in murine retrovirus-induced AIDS inhibit T- and B-cell responses *in vitro* that are used to define the immunodeficiency. J Virol **87:**2058–2071. http://dx.doi.org/10.1128/JVI.01547-12.
70. **O'Connor MA, Vella JL, Green WR.** 2016. Reciprocal relationship of T regulatory cells and monocytic myeloid-derived suppressor cells in LP-BM5 murine retrovirus-induced immunodeficiency. J Gen Virol **97:**509–522. http://dx.doi.org/10.1099/jgv.0.000260.
71. **Green KA, Wang L, Noelle RJ, Green WR.** 2015. Selective involvement of the checkpoint regulator VISTA in suppression of B-cell, but not T-cell, responsiveness by monocytic myeloid-derived suppressor cells from mice infected with an immunodeficiency-causing retrovirus. J Virol **89:**9693–9698. http://dx.doi.org/10.1128/JVI.00888-15.
72. **O'Connor MA, Fu W, Green KA, Green WR.** 2015. Subpopulations of M-MDSCs from mice infected by an immunodeficiency-causing retrovirus and their differential suppression of T- vs B-cell responses. Virology **485:**263–273. http://dx.doi.org/10.1016/j.virol.2015.07.020.